Measurements of Thermal Rate Constants for the Reactions of $N(^2D,^2P)$ with C_2H_4 and C_2D_4 between 225 and 292 K

Kei Sato, Kazuaki Misawa, Yasuhide Kobayashi, Miho Matsui, and Shigeru Tsunashima*

Department of Applied Physics, Tokyo Institute of Technology, Ookayama, Meguro-ku, Tokyo 152-8551, Japan

Yuzuru Kurosaki and Toshiyuki Takayanagi

Advance Science Research Center, Japan Atomic Energy Research Institute, Tokai-mura, Naka-gun, Ibaraki 319-1195, Japan

Received: May 26, 1999; In Final Form: August 16, 1999

The thermal rate constants for the reactions of electronically excited nitrogen atoms, $N(^2D)$ and $N(^2P)$, with C_2H_4 and C_2D_4 have been measured by using a pulse radiolysis−atomic absorption method between 225 and 292 K. From the results of the kinetic isotope effect for the $N(^2D)$ reaction, a main reaction mechanism was assigned to be the N addition to the double bond. This conclusion is in accordance with the prediction of our previous ab initio calculations. Variational transition-state theory calculations were performed for the $N(^2D)$ reaction by using the results of ab initio molecular orbital calculations. It was suggested that correction of the "multiple surface coefficient" is necessary to interpret the measured rate constants. The ratio of the rate constant of $N(^2D)$ to that of $N(^2P)$ was found to be close to unity and was much smaller than those for the reactions with H_2 and CH_4. The deactivation process of $N(^2P)$ was determined to be the spin-allowed quenching process, $N(^2P) + C_2H_4(S_0) \rightarrow N(^4S) + C_2H_4(T_1)$.

1. Introduction

The reactions of atomic nitrogen in the electronically ground and excited states with hydrocarbon molecules are considered to be important in the atmosphere of Titan,[1] the interstellar cloud,[2] and the hydrocarbon combustion.[3] These reactions have traditionally been investigated in laboratories by using "active nitrogen" containing atomic and molecular nitrogen in the electronically ground and excited states.[4,5] Early workers believed that the reaction of ground-state atom with stable hydrocarbons is an important initiation step in the presence of "active nitrogen."[6−9] However, this reaction scheme was contradicted from later kinetic studies by Michael et al.[10−12] and this laboratory.[13] The important step is now considered to be the reaction of the excited-state molecule[5] and/or atom[14−16] followed by the reaction of the ground-state atom with free radicals.[17−21]

The detailed mechanisms and dynamics of reactions of the excited nitrogen atoms, $N(2p^3\ ^2D$; 54.9 kcal mol^{-1} above ground $^4S)$ and $N(2p^3\ ^2P$; 82.4 kcal mol^{-1} above $^4S)$, have recently been studied thanks to the development of experimental techniques. Umemoto et al. measured the nascent rotational state distribution of the NH product for reactions of $N(^2D)$ with H_2, CH_4, C_2H_6, and C_3H_8 by using two-photon photolysis of NO.[22−26] Casavecchia and co-workers measured the product angular distributions for reactions of $N(^2D)$ with H_2 and C_2H_2 by using supersonic beam of excited nitrogen atom.[27−29] Very recently, Bakker et al. succeeded in producing velocity aligned $N(^2D)$ using two-color laser photolysis of NO and discussed the possibility of studying the reactions of monoenergetic velocity aligned atoms.[30] Our group has measured the temperature dependence of the rate constants and kinetic isotope effects for the reactions of $N(^2D,^2P)$ with H_2, C_2H_2, and CH_4 to obtain the information on potential energy barrier.[31−33] From the theoretical side, our group has performed ab initio molecular orbital (MO) calculations for the reactions of $N(^2D)$ with H_2, CH_4, C_2H_2, and C_2H_4 to predict reaction mechanism and products.[33−36] Pederson et al. also studied the potential energy surface of the reaction of $N(^2D)$ with H_2 using the ab initio MO method.[37]

The reaction of $N(^2D)$ with CH_4 has been suggested to proceed via the insertion of N atom into the CH bond:[25,32]

$$N(^2D) + CH_4 \rightarrow CH_3NH \rightarrow \text{products} \qquad (1)$$

while the reaction with C_2H_2 has been suggested to proceed via the addition of N atom to the triple bond:[33]

$$N(^2D) + HC{\equiv}CH \longrightarrow \underset{\displaystyle N}{HC{=}CH} \longrightarrow \text{products} \qquad (2)$$

For the reaction with C_2H_4, both the insertion to the CH bond and addition to the double bond are possible. In our previous study,[36] the barrier heights of these processes were estimated using the ab initio MO method. The barrier height of the addition to the double bond was estimated to be much smaller than that of the insertion into CH bond. The rate constant was calculated on the basis of conventional transition state theory (TST) and was compared with the observed values at room temperature. However, due to overestimation of the barrier height, only the qualitative discussion was performed. In order to obtain information on the barrier height, measurements of the temperature dependence of the rate constant are necessary.

In this paper, we present measurements of the rate constants for reactions of $N(^2D,^2P)$ with C_2H_4 and C_2D_4 between 225 and 292 K using pulse radiolysis technique combined with the

* Corresponding author.

10.1021/jp991742l CCC: $18.00
Published on Web 10/14/1999

atomic absorption method. The experimental results of such measurements may provide information not only on the barrier height but also on the reaction pathway.[32,33] From a comparison of the measured temperature dependence of the rate constant with that of the calculated rate constants for the $N(^2D)$ reaction, the reaction dynamics can be discussed in detail. In this study, canonical variational transition-state theory (VTST), which is more accurate than conventional TST, is employed. Reaction mechanism of $N(^2P)$ is also discussed.

2. Experimental Section

A method of pulse radiolysis−atomic absorption was employed to measure the temperature dependence of the rate constant. The procedure was similar to that described elsewhere.[31−33] Briefly, a mixture of N_2 and C_2H_4 (C_2D_4) in a stainless steel vessel was irradiated by a pulsed electron beam from a Febetron 706 apparatus (Hewlett-Packard) to produce $N(^2D)$ and $N(^2P)$. The concentration of $N(^2D)$ and $N(^2P)$ was monitored by using the atomic absorption lines at 149 nm ($2p^2\ 3s\ ^2P-2p^3\ ^2D$) and 174 nm ($2p^2\ 3s\ ^2P-2p^3\ ^2P$), respectively. The atomic lines were derived from a microwave discharge in a flow of N_2/He. Transmitted light was detected with a photomultiplier tube (Hamamatsu, R976) through a vacuum−UV monochromator (Shimadzu, SGV-50). Since the optical density used for the present study was less than 0.5, Lambert−Beer's law approximately holds.[38,39] The signal was amplified and processed with a wave memory (NF Circuit Design Block, WM-862) and a personal computer (NEC, PC-9801RX). Since the spin−orbit fine structures of atomic lines could not be resolved under the present experimental condition, the measured rate constant is averaged over spin−orbit sublevels. For the measurement of $N(^2P)$, the typical pressure of N_2 was kept at 700 Torr, while the C_2H_4 (C_2D_4) pressure was varied between 0 and 20 mTorr. For the measurement of $N(^2D)$, the gas mixture was diluted with He because $N(^2D)$ is efficiently deactivated by N_2.[31] Typical pressures of C_2H_4 (C_2D_4), N_2, and He were 0−20 mTorr, 1 Torr, and 700 Torr, respectively. The charging voltage of Febetoron was varied in the range of 24−26 kV to check the effect of the radiolysis of C_2H_4 (C_2D_4). The measured rate constant was found to be independent of the voltage in this range. The initial concentration of $N(^4S)$ was previously estimated to be an order of 10^{13} molecule cm^{-3}.[39] The concentration of $N(^2D,^2P)$ should be much smaller than that of $N(^4S)$ and that of C_2H_4 (C_2D_4). For example, the typical concentration of ^2D was roughly estimated to be $10^{11}-10^{12}$ molecules cm^{-3}. Thus, the pseudo-first-order approximation holds under the present experimental condition. C_2H_4 (purchased from Takachiho Shoji) and C_2D_4 (ICON) were used after bulb to bulb distillations. N_2 (Taiyo-Toyo Sanso) and He (Union Helium) were used after passing through heated reduced copper chips and liquid nitrogen trap.

3. Results and Discussion

Rate Measurements. The temporal curve of the concentration of $N(^2D)$ and $N(^2P)$ could be fitted with a single-exponential curve. This means that the concentration of $N(^2D)$ and $N(^2P)$ decreases via the pseudo-first-order decay mechanism. The decay rate was calculated by using a nonlinear least-squares fitting method. A typical plot of the decay rate as a function of the C_2H_4 pressure is shown in Figure 1. Each experimentally determined decay rate has an error of ∼10%. The decay rate was independent of the total pressure in the range between 600 and 700 Torr. The rate constant can be obtained from the slope of the straight line. Table 1 summarizes the rate constants

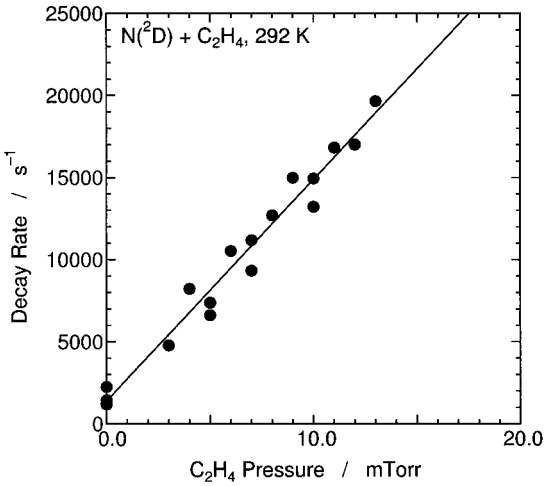

Figure 1. A typical plot of the decay rate as a function of the C_2H_4 pressure for $N(^2D) + C_2H_4$ at 292 K. Straight line is a result of linear fitting.

TABLE 1: Measured Rate Constant for the Reactions of $N(^2D)$ and $N(^2P)$ with C_2H_4 and C_2D_4

reaction	T/K	$k/10^{-11}$ cm^3 $molecule^{-1}$ s^{-1}
present results		
$N(^2D) + C_2H_4$	292	4.1 ± 0.4
	270	3.4 ± 0.4
	253	3.0 ± 0.4
	240	2.8 ± 0.4
	230	2.6 ± 0.4
$N(^2D) + C_2D_4$	292	3.4 ± 0.6
	270	3.0 ± 0.6
	253	2.4 ± 0.4
	240	2.2 ± 0.4
	230	2.1 ± 0.4
$N(^2P) + C_2H_4$	292	3.1 ± 0.3
	272	2.5 ± 0.3
	252	2.1 ± 0.4
	233	2.1 ± 0.4
	225	1.9 ± 0.3
$N(^2P) + C_2D_4$	292	2.9 ± 0.4
	253	2.3 ± 0.4
	240	2.1 ± 0.4
literature values		
$N(^2D) + C_2H_4$	300	12[a]
$N(^2D) + C_2H_4$	300	8.3 ± 2.5[b]
$N(^2P) + C_2H_4$	295	3.1 ± 0.4[c]

[a] Reference 14. [b] Reference 15. [c] Reference 16.

measured for the reactions of $N(^2D, ^2P)$ with C_2H_4 and C_2D_4 with the error of one standard deviation. The rate constants are also compared to literature values in Table 1. Black et al. estimated the rate constant for the $N(^2D) + C_2H_4$ reaction at 300 K by analyzing the time variation of intensity of NO(β) emission observed in the 147 nm photolysis of N_2O at a total pressure of 3−10 Torr.[14] Their result is 1.2×10^{-10} cm^3 $molecule^{-1}$ s^{-1} and is about 3 times as large as the present result at room temperature. Fell et al. also measured the rate constant at 300 K using a combination of discharge flow method and electron spin resonance technique at a total pressure of 4−8 Torr.[15] Their result corrected for the laminar flow is $(8.3 \pm 2.5) \times 10^{-11}$ cm^3 $molecule^{-1}$ s^{-1} and is closer to the present result than the result by Black et al. The rate constant for the reaction of $N(^2P)$ with C_2H_4 at room temperature has previously been measured in this laboratory.[16] The previous result at room temperature shows good agreement with the present results. The temperature dependence of the measured rate constants is found to be well reproduced by the Arrhenius equation as shown in

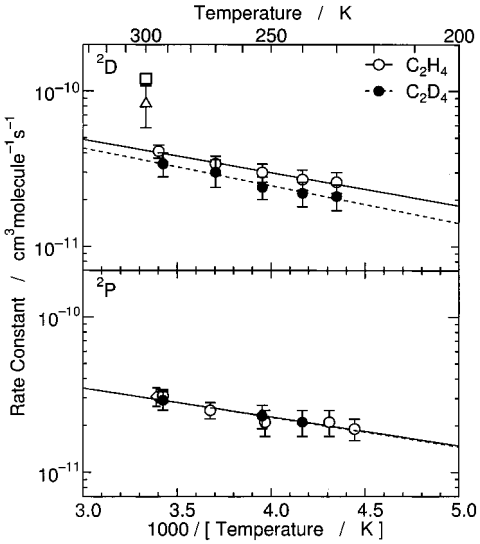

Figure 2. Arrhenius plot for the N(^{2}D) reactions (upper panel) and that for the N(^{2}P) reactions (lower panel). Open and closed circles are the corresponding experimental results for C_2H_4 and C_2D_4, respectively. Straight lines are fitted results obtained by using nonlinear least-squares method. Previous experimental results are also included: (□) ref 14, (△) ref 15, and (◇) ref 16.

TABLE 2: Arrhenius Parameters for the Reactions of N(^{2}D) and N(^{2}P) with Simple Hydrocarbon Molecules

reaction	A/cm^3 molecule^{-1} s^{-1}	E_a/kcal mol^{-1}	ref
reactions of N(^{2}D)			
N(^{2}D) + C_2H_4	$(2.3 \pm 0.3) \times 10^{-10}$	1.0 ± 0.1	this work
N(^{2}D) + C_2D_4	$(2.4 \pm 0.5) \times 10^{-10}$	1.1 ± 0.1	this work
N(^{2}D) + CH_4	$(7.1 \pm 4.4) \times 10^{-11}$	1.5 ± 0.3	32
N(^{2}D) + CD_4	$(3.3 \pm 1.4) \times 10^{-11}$	1.4 ± 0.1	32
N(^{2}D) + C_2H_2	$(1.6 \pm 0.2) \times 10^{-10}$	0.53 ± 0.06	33
N(^{2}D) + C_2D_2	$(1.4 \pm 0.1) \times 10^{-10}$	0.48 ± 0.05	33
reactions of N(^{2}P)			
N(^{2}P) + C_2H_4	$(1.4 \pm 0.5) \times 10^{-10}$	0.91 ± 0.18	this work
N(^{2}P) + C_2D_4	$(1.3 \pm 0.2) \times 10^{-10}$	0.87 ± 0.10	this work
N(^{2}P) + CH_4	$(5.0 \pm 2.2) \times 10^{-13}$	0.98 ± 0.22	32
N(^{2}P) + CD_4	$(3.1 \pm 1.4) \times 10^{-13}$	0.96 ± 0.24	32
N(^{2}P) + C_2H_2	$(1.0 \pm 0.1) \times 10^{-10}$	0.88 ± 0.06	33
N(^{2}P) + C_2D_2	$(0.71 \pm 0.12) \times 10^{-10}$	0.76 ± 0.09	33

[a] Error represents one standard deviation.

Figure 2. The Arrhenius parameters are summarized in Table 2. The activation energies are about 1 kcal mol^{-1} for both the N(^{2}D) + C_2H_4 and N(^{2}D) + C_2D_4 reactions. The activation energies for the reactions of N(^{2}P) are also close to those for N(^{2}D). The ratios of the rate constant of C_2H_4 to that of C_2D_4 for N(^{2}D) and N(^{2}P) were ~1.2 and ~1.0, respectively.

Figure 3 shows the temperature dependence of the ratio of the rate constant for the reaction of N(^{2}D) with hydrocarbon to that for the reaction with its isotopic variant, k_H/k_D, for the reactions with C_2H_4, CH_4,[32] and C_2H_2.[33] It is seen that the ratio of k_H/k_D was independent of temperature for these reactions. The average of k_H/k_D for C_2H_4 was 1.2 ± 0.2. For CH_4, the average of k_H/k_D was 1.7 ± 0.2. As described previously, the reaction with methane is considered to be insertive into a CH bond.[32,34] The motion along reaction coordinate around the transition state of insertion reaction contains the hydrogen migration.[34] Thus, a large kinetic isotope effect is expected for the reaction with CH_4. For C_2H_2, the average of k_H/k_D was 1.0 ± 0.1. The reaction with acetylene is considered to be additive to the CC triple bond.[33] The motion along the reaction coordinate around the transition state of the addition reaction is mainly relative translation between N and C_2H_2 and does not contain

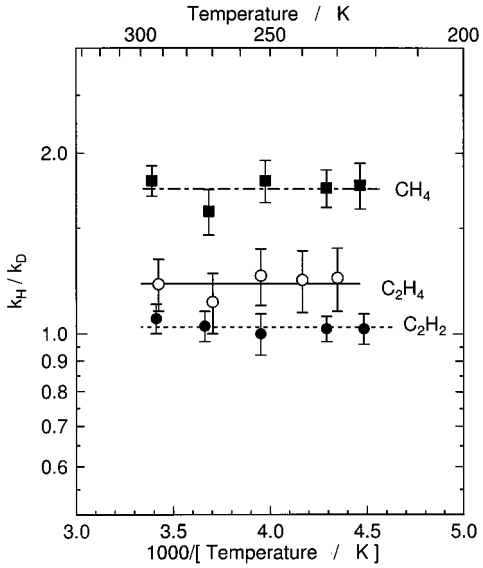

Figure 3. Kinetic isotope effect for the reactions of N(^{2}D) with CH_4, C_2H_2, and C_2H_4 as a function of temperature. k_H and k_D are the rate constants for the reactions with hydrocarbon and its deuterated variant, respectively.

hydrogen migration.[33] Therefore, less or no kinetic isotope effect was expected for the reaction with C_2H_2. It is then noted that k_H/k_D can be a sensitive check for the reaction mechanism. For the reaction of N(^{2}D) with C_2H_4, the barrier height of the hydrogen abstraction was predicted to be high.[36] Thus, the insertion of N into the CH bond of C_2H_4 and the addition of N to the CC double bond are possible reaction pathways. The average of k_H/k_D was 1.2 ± 0.2 and was close to the result of C_2H_2. This strongly suggests that the reaction with C_2H_4 proceeds via the addition reaction to form the cyclic intermediate.[36]

Table 2 compares the Arrhenius parameters measured in the present study with those measured in the previous study of the reactions with CH_4[32] and C_2H_2.[33] The A factor of addition reaction of N(^{2}D) with C_2H_2 is about twice as large as that of insertion reaction with CH_4. The A factor measured for C_2H_4 is close to that measured for C_2H_2 rather than CH_4 as listed in Table 2. This also supports the above conclusion that the reaction of C_2H_4 is additive in analogy with that of C_2H_2.

It is interesting to compare the N(^{2}D) + C_2H_4 reaction with the reactions between other species and C_2H_4. For the isoelectronic reaction of CH($^2\Pi$) with C_2H_4, the rate constant at room temperature was measured to be $(2.1-4.2) \times 10^{-10}$ cm^3 molecule^{-1} s^{-1} and the activation energy was found to be close to zero and negative.[40,41] This is in contrast to the present result of the positive activation energy for the N(^{2}D) reaction. For the CH + C_2H_4 reaction, both the addition of CH radical to the double bond and the insertion of CH radical into ethylene CH bond are also possible. The barrier heights for these processes were studied by ab initio MO calculations.[42] It was predicted that the barrier for the addition is much lower than that for the insertion. The reaction mechanism for CH radical is similar to that for N(^{2}D) atom. For the CH addition, no potential energy barrier was predicted to exist in agreement with the experimental data of the small negative activation energy.

The O(^{1}D) + C_2H_4 reaction is also compared with the N(^{2}D) + C_2H_4 reaction. The rate constant at room temperature for the reaction of O(^{1}D) was reported to be[43] $(2.2 \pm 0.5) \times 10^{-10}$ cm^3 molecule^{-1} s^{-1} and is about 5 times as large as that for the reaction of N(^{2}D). This may mainly be caused by the fact that the activation energy of the reaction of O(^{1}D) is much smaller

than that of the reaction of $N(^2D)$, ~1 kcal mol^{-1}. It has traditionally been believed that the reaction of $O(^1D)$ with olefin proceeds via the concerted addition of O atom to the double bond.[44] The insertion of O atom to the CH bond is also considered to be possible from the laser-induced fluorescence measurements of the product OH radical.[45,46] In contrast to this, Umemoto et al. found that NH radical was not detected as a product of the $N(^2D) + C_2H_4$ reaction[47] though they succeeded in detecting the NH product for the $N(^2D) + CH_4$ reaction.[24] These suggest that both the insertion and addition reactions are competitive for the $O(^1D)$ reaction, but only the addition reaction is possible for the $N(^2D)$ reaction.

VTST Calculation for $N(^2D)$ Reaction. In order to discuss quantitatively the temperature dependence of the rate constants for the $N(^2D)$ reaction, canonical VTST calculations have been carried out. In the canonical VTST, the rate constant, $k(T)$, is determined so as that the rate constant of generalized transition-state (GT) is minimized as a function of reaction coordinate s:[48]

$$k(T) = \min k^{GT}(T,s) \tag{I}$$

where

$$k^{GT}(T,s) = f_e \Gamma L \frac{k_B T}{h} \frac{Q^{GT}(T,s)}{Q_r(T)} e^{-V(s)/k_B T} \tag{II}$$

Here $k^{GT}(T,s)$ is the rate constant of GT. Γ and L are the tunneling correction factor and reaction path degeneracy, respectively. $Q_r(T)$ and $Q^{GT}(T,s)$ are the partition functions for the reactant and GT, respectively. f_e is the multiple surface coefficient. Note that the partition functions exclude electronic degrees of freedom. In the traditional treatments, f_e is the ratio of electronic partition function of GT to that of reactant. If only the lowest doublet potential energy surface leads to reaction, f_e should approximately be 0.2 because five doublet surfaces asymptotically correlate to $N(^2D) + C_2H_4$. However, if nonadiabatic transition among these five doublet surfaces is important, f_e is in the range of 0.2−1.0. This will be further discussed below.

All the information needed for the VTST calculations was obtained by the ab initio MO method. The intrinsic reaction coordinate (IRC) for the addition of N atom to the CC double bond of C_2H_4 was calculated at the CASSCF(5,5)/cc-pVDZ level of theory. The active orbitals were the same as those employed in our previous paper.[36] Five electrons were distributed among three nitrogen 2p orbitals and CC π and π^* orbitals. It was predicted from the IRC analysis that the reaction proceeds via the perpendicular approach of N atom to the C_2H_4 plane and the transition state is very loose. In other words, for the transition state the distance between N atom and the center of mass of C_2H_4 is very long (about 2.8 Å) and the molecular geometry of C_2H_4 moiety is very similar as that of free C_2H_4. The projected harmonic vibrational frequencies along s were also obtained at the same level of theory as that employed for the IRC calculations. These CASSCF calculations were performed using the Gaussian 94 package programs.[49] Figure 4 shows the vibrational frequencies, rotational constants, and potential energies as a function of s for the reaction with C_2H_4, where the absolute value of s is the arc length of the IRC measured from the transition state. Similar results were obtained for the reaction with C_2D_4. The classical barrier height was calculated to be 3.2 kcal mol^{-1} at the CASSCF(5,5)/cc-pVDZ level of theory, which is larger than the experimentally obtained Arrhenius activation energy, ~1 kcal mol^{-1}. This is not surprising since the CASSCF-level calculation is not very accurate for estimating the classical barrier height. This is primarily due to the fact that the CASSCF method does not include the effect of dynamical electron correlation. Therefore, the potential energies have been calculated at a more accurate level of theory than the CASSCF level along the IRC path. The level of theory used was the second-order configuration interaction (SOCI) method, which uses the CASSCF(5,5) configurations as reference ones. The cc-pVDZ basis set was also used in the SOCI calculations. Since C_s symmetry was assumed, the actual numbers of configuration-state functions were about 55 000 for both A' and A'' symmetry. The SOCI calculations were carried out by using the HONDO7 program.[50] The result of the SOCI calculations along s is also included in Figure 4. The calculated classical barrier height for the SOCI calculation was much smaller than that for the CASSCF calculation. The corresponding potential energy curve has a maximum of 0.7 kcal mol^{-1} at $s = -1.1$ amu$^{1/2}$ bohr.

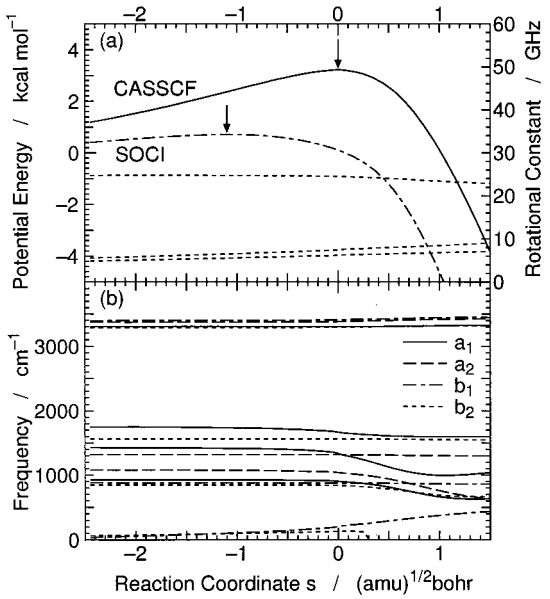

Figure 4. Molecular constants along the IRC path calculated at the CASSCF/cc-pVDZ level and the potential energy curves calculated at the CASSCF/cc-pVDZ and SOCI/cc-pVDZ levels for the reaction of $N(^2D)$ with C_2H_4: (a) potential energy calculated at the CASSCF/cc-pVDZ level (—), potential energy calculated at the SOCI/cc-pVDZ level (- - -) and rotational constants (— - —) and (b) harmonic vibrational frequencies in a_1 (—), a_2 (— — —), b_1 (— - —), and b_2 (---) symmetries.

The results of the VTST calculations are presented in Figure 5. In the VTST calculations, the harmonic vibrational frequencies along s were multiplied by a correction factor of 0.94. This correction factor was evaluated by comparing the calculated vibrational frequencies for C_2H_4 and C_2D_4 with those of experimental results.[51] However, effects of this correction on the rate constants were found to be very small. The b_1 mode with the lowest frequency was treated as a hindered rotation rather than vibration since the transition state of the addition reaction was predicted to be very loose and this mode was assigned to be the internal rotation of C_2H_4 moiety about the CC double bond. The equation proposed by Troe was used to calculate the partition function of this mode.[52] The tunneling-correction factor was estimated to be 1.1−1.2 by using the Wigner's method.[53] Curves (a) in Figure 5 are the VTST results with $f_e = 0.2$, in which the CASSCF potential energy profile is used. The calculated rate constants are much smaller than the measured ones due to the large classical barrier height. The rate constants calculated by using the SOCI potential energy profile

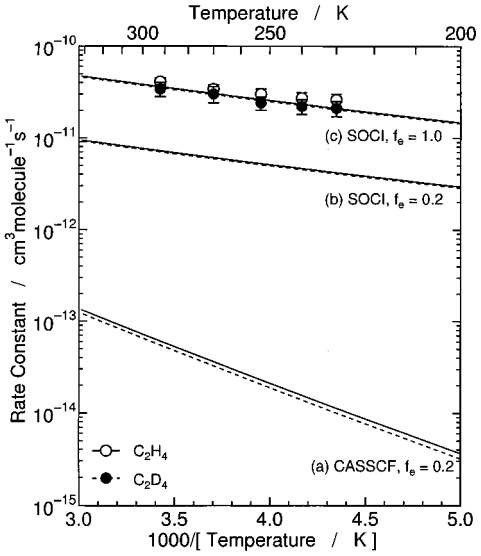

Figure 5. Comparison of the measured rate constants with those evaluated from VTST calculations for the reactions of N(^{2}D) with C_2H_4 and C_2D_4. Open circles are the experimental results for C_2H_4. Closed circles are the experimental results for C_2D_4. Solid curves are VTST results for C_2H_4. Dotted curves are VTST results for C_2D_4. For details of the VTST calculations, see text.

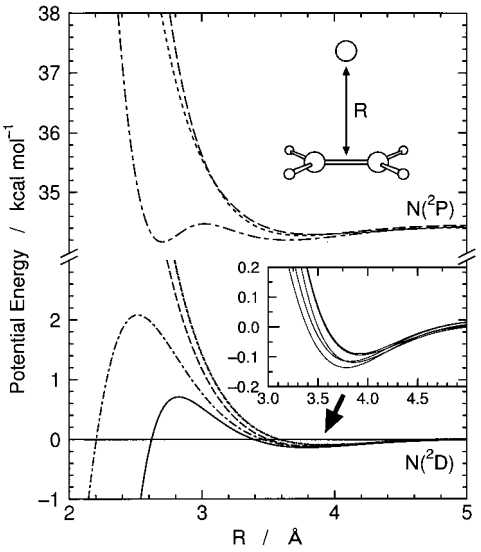

Figure 6. Ab initio potential energies for lowest eight doublet states which asymptotically correlate to N(^{2}D) + C_2H_4 and N(^{2}P) + C_2H_4 as a function of the distance between N and the center-of-mass of C_2H_4. The inserted figure is an expansion of the potential energies in a van der Waals region.

are also plotted in Figure 5. Curves (b) and (c) are the results with $f_e = 0.2$ and $f_e = 1$, respectively. Solid and dotted lines in Figure 5 represent the results for C_2H_4 and C_2D_4, respectively. It is seen that the calculated results of kinetic isotope effect are very small for all the cases of (a)−(c) in agreement with the experimental data. Excellent agreement can be seen between curves (c) and experimental rate constants. This suggests that nonadiabatic transition occurs much more rapidly than the addition reaction and the transition to the lowest reactive surface is efficient in the reaction of N(^{2}D) with C_2H_4.

In order to discuss qualitatively the importance of nonadiabatic transitions, the potential energy curves were calculated at the SOCI/cc-pVDZ level of theory. Figure 6 shows the lowest eight doublet potential curves as a function of the distance between N and the center of mass of C_2H_4. Only a perpendicular

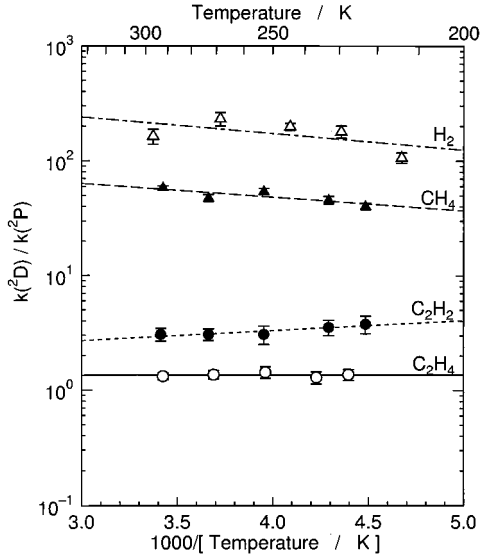

Figure 7. Ratios of rate constant of N(^{2}D) to that of N(^{2}P) for the reactions with H_2, CH_4, C_2H_2, and C_2H_4.

approach of N to the molecular plane of C_2H_4 was considered. The molecular geometries were confined within C_{2v} symmetry. The geometry of the C_2H_4 moiety was kept in that of free ethylene. The lowest five potential curves asymptotically correlate to the N(^{2}D) state and the other three curves to the N(^{2}P) state. Shallow van der Waals wells are seen to exist in all the potential curves at 3.8 Å. The several crossing points are seen in the van der Waals region. Note that these crossings become avoided ones when the molecular geometry reduces to C_1 symmetry. This suggests that nonadiabatic transitions are important in this region. For five potential curves correlating to the N(^{2}D) state, the lowest one was found to have the lowest energy barrier. This result also suggests that the transition to the lowest reactive surface is efficient.

Very recently, Schatz and co-workers have performed accurate three-dimensional quantum reactive scattering calculations for the Cl(^{2}P$_{3/2,1/2}$) + HCl reaction.[54] They have included the three electronically coupled potential energy surfaces obtained from ab initio calculations and discussed the effect of nonadiabatic transitions on thermal rate constant by changing artificially the magnitude of spin−orbit interaction. When the spin−orbit energy splitting is larger than the depth of van der Waals well, the dynamics is predominantly adiabatic. When the energy splitting is much smaller than the depth of the van der Waals well, nonadiabatic transitions significantly occur in the van der Waals regions. The depth of van der Waals wells between N(^{2}D) and C_2H_4 can roughly be estimated to be about 0.1 kcal mol^{-1} from the SOCI results in Figure 5. This value is much larger than the spin−orbit energy splitting between N(^{2}D$_{5/2}$) and N(^{2}D$_{3/2}$), 8.7 cm^{-1} = 0.025 kcal mol^{-1}.[55] Thus, it is probable that the nonadiabatic transition plays an important role at van der Waals wells in the reaction of N(^{2}D) with C_2H_4.

N(^{2}P) Reaction. Figure 7 shows a plot of the ratio of k(^{2}D)/k(^{2}P) as a function of temperature for the reaction with H_2, CH_4, C_2H_2, and C_2H_4. For the reaction with H_2, the ratio of k(^{2}D)/k(^{2}P) is 1×10^2 to 2×10^2. It was considered that the N(^{2}D) + H_2 reaction proceeds via the chemical reaction whereas the N(^{2}P) + H_2 reaction proceeds via the nonadiabatic physical quenching to N(^{2}D) or N(^{4}S) from discussion based on the correlation diagram for the reactions of N(^{2}D) and N(^{2}P).[14,31] This may be the reason why the rate constant is much smaller than that for N(^{2}D). The ratio of k(^{2}D)/k(^{2}P) for the reaction of CH_4 is 40−60 and is similar to the results for H_2. The same

explanation as the H_2 case is also possible.[32] These results strongly suggest that the reaction mechanisms of $N(^2D)$ and $N(^2P)$ are entirely different. The ratio of $k(^2D)/k(^2P)$ for C_2H_2 is about 3 and is much smaller than those for H_2 and CH_4. Another quenching process such as $N(^2P) + C_2H_2(S_0) \rightarrow N(^4S) + C_2H_2(T_1)$ for unsaturated C_2H_2 is one of possible reaction mechanisms to explain the experimental results.[33] For the reaction with C_2H_4, $k(^2D)/k(^2P)$ is close to unity and is smaller than the results of C_2H_2. A similar quenching process as that for C_2H_2

$$N(^2P) + C_2H_4(S_0) \rightarrow N(^4S) + C_2H_4(T_1) \qquad (3)$$

can also be considered for C_2H_4. By using the S_0-T_1 energy difference calculated by Gemein[56] and experimental value of the $^2P-^4S$ energy difference,[55] the exoergicity is calculated to be 19.9 kcal mol^{-1}. This result indicates that reaction 3 is energetically possible. The energy difference between the S_0 and T_1 states for ethylene, 62.5 kcal mol^{-1},[56] is smaller than that for acetylene, 80.6−88.7 kcal mol^{-1},[57] because the triplet excited ethylene can be electronically stabilized by the CH_2 rotation about the double bond. The exoergicity for reaction 3 is larger than that of the corresponding reaction for acetylene. Reaction 3 can be tentatively assigned to be a deactivation process of $N(^2P)$ by C_2H_4. As shown in Figure 2, no kinetic isotope effect was observed for the $N(^2P)$ reaction. This is consistent with the above assignment for the $N(^2P) + C_2H_4$ reaction. The possibility of chemical reaction channels cannot be ruled out as a deactivation process of $N(^2P)$ because the initial product of the $N(^2P) + C_2H_4$ reaction has not been directly detected in the present study. In order to understand the deactivation process of $N(^2P)$, further experimental studies are necessary.

As listed in Table 2, the activation energy for the $N(^2P) + C_2H_4$ reaction was determined to be about 0.9 kcal mol^{-1}. The results of the present ab initio MO calculations showed that the lowest potential energy curve which correlates to $N(^2P) + C_2H_4$ has the potential energy barrier at the $N-C_2H_4$ distance of 3 Å as shown in Figure 6. This is consistent with the experimental results of the positive activation energy. It is also necessary to study further the doublet and quartet potential energy surfaces at various molecular geometries and to find the crossing points because the physical quenching may proceed via such crossing points.

4. Conclusions

Thermal rate constants for $N(^2D,^2P) + C_2H_4$ (C_2D_4) were measured using a technique of pulse radiolysis−atomic absorption between 225 and 292 K. Arrhenius parameters were determined from the temperature dependence of the rate constants. The ratio of k_H/k_D was close to unity for the reactions of $N(^2D)$. This small kinetic isotope effect suggests that the reaction of $N(^2D)$ proceeds mainly via the addition of N atom to the double bond. The canonical VTST calculations have been carried out for the $N(^2D)$ reaction by using the ab initio results of IRC path obtained at the SOCI/cc-pVDZ//CASSCF(5,5)/cc-pVDZ level. The comparison between the calculated and measured rate constants suggests that the "multiple surface coefficient" is much larger than the statistical value, 0.2. This indicates that nonadiabatic transitions in the van der Waals regions play an important role in the collision dynamics between $N(^2D)$ and C_2H_4. The rate constant for the reactions of $N(^2P)$ was found to be close to that for the reactions of $N(^2D)$. One of the deactivation processes of $N(^2P)$ is physical quenching, $N(^2P) + C_2H_4(S_0) \rightarrow N(^4S) + C_2H_4(T_1)$, although the contribution of chemical reactions cannot be ruled out. In order to understand the deactivation mechanism of $N(^2P)$, further experimental and theoretical studies are necessary.

Acknowledgment. K.S. thanks Professor Umemoto of Japan Advanced Institute of Science and Technology for helpful discussion and supplying experimental data prior to the publication. K.S. also thanks the reviewers for carefully reading the manuscript and pointing out typographical errors.

References and Notes

(1) Yung, Y. L.; Allen, M. A.; Pinto, J. P. *Astrophys. J. Suppl. Ser.* **1984**, *55*, 465.
(2) Langer, W. D.; Graedel, T. E. *Astrophys. J. Suppl. Ser.* **1989**, *69*, 241.
(3) Miller, J. A.; Bowman, C. T. *Prog. Energ. Combust. Sci.* **1989**, *15*, 287.
(4) Brocklehurst, B.; Jennings, K. R. *Prog. React. Kinet.* **1967**, *4*, 1.
(5) Safrany, D. R. *Prog. React. Kinet.* **1971**, *6*, 1.
(6) Herron, J. T. *J. Phys. Chem.* **1965**, *69*, 2786.
(7) Herron, J. T. *J. Phys. Chem.* **1966**, *70*, 2803.
(8) Herron, J. T.; Huie, R. E. *J. Phys. Chem.* **1968**, *72*, 2538.
(9) Sato, S.; Sugawara, K.; Ishikawa, Y. *Chem. Phys. Lett.* **1979**, *68*, 557.
(10) Michael, J. V.; Lee, J. H. *Chem. Phys. Lett.* **1977**, *51*, 303.
(11) Michael, J. V. *Chem. Phys. Lett.* **1979**, *68*, 561.
(12) Michael, J. V. *Chem. Phys. Lett.* **1980**, *76*, 129.
(13) Umemoto, H.; Nakagawa, S.; Tsunashima, S.; Sato, S. *Bull. Chem. Soc. Jpn.* **1986**, *59*, 1449.
(14) Black, G.; Slanger, T. G.; St. John, G. A.; Young, R. A. *J. Chem. Phys.* **1969**, *51*, 116.
(15) Fell, B.; Rivas, I. V.; McFadden, D. L. *J. Phys. Chem.* **1981**, *85*, 224.
(16) Umemoto, H.; Sugiyama, K.; Tsunashima, S., Sato, S. *Bull. Chem. Soc. Jpn.* **1985**, *58*, 3076.
(17) Stief, L. J.; Marston, G.; Nava, D. F.; Payne, W. A.; Nesbitt, F. L. *Chem. Phys. Lett.* **1989**, *147*, 570.
(18) Marston, G.; Nesbitt, F. L.; Nava, D. F.; Payne, W. A.; Stief, L. J. *J. Phys. Chem.* **1989**, *93*, 5769.
(19) Marston, G.; Nesbitt, F. L.; Stief, L. J. *J. Chem. Phys.* **1989**, *91*, 3483.
(20) Stief, L. J.; Nesbitt, F. L.; Payne, W. A. Tao, W.; Kuo, S. C.; Klemm, R. B. *J. Chem. Phys.* **1995**, *102*, 5309.
(21) Payne, W. A.; Monks, P. S.; Nesbitt, F. L.; Stief, L. J. *J. Chem. Phys.* **1996**, *104*, 9808.
(22) Umemoto, H.; Matsumoto, K. *J. Chem. Soc., Faraday Trans.* **1996**, *92*, 1315.
(23) Umemoto, H.; Asai, T.; Kimura, Y. *J. Chem. Phys.* **1997**, *106*, 4985.
(24) Umemoto, H.; Kimura, Y.; Asai, T. *Chem. Phys. Lett.* **1997**, *264*, 215.
(25) Umemoto, H.; Kimura, Y.; Asai, T. *Bull. Chem. Soc. Jpn.* **1997**, *70*, 2951.
(26) Umemoto, H. *Chem. Phys. Lett.* **1998**, *292*, 594.
(27) Alagia, M.; Aquilanti, V.; Ascenzi, D.; Balucani, N.; Cappelletti, D.; Cartechini, L.; Casavecchia, P.; Pirani, F.; Sancini, G.; Volpi, G. G. *Isr. J. Chem.* **1997**, *37*, 329.
(28) Alagia, M.; Balucani, N.; Cartchini, L.; Casavecchia, P.; Volpi, G. G.; Pederson, L. A.; Schatz, G. C.; Lendvay, G.; Harding, L. B.; Hollebeek, T.; Ho, T.-S.; Rabitz, H. *J. Chem. Phys.* **1999**, *110*, 8857.
(29) Alagia, M.; Balucani, N.; Cartchini, L.; Casavecchia, P.; Volpi, G. G.; Sato, K.; Takayanagi, T.; Kurosaki, Y. Submitted for publication.
(30) Bakker, B. L. G.; Eppink, A. T. J. B.; Parker, D. H.; Costen, M. L.; Hancock, G.; Ritchie, G. A. D. *Chem. Phys. Lett.* **1998**, *283*, 319.
(31) Suzuki, T.; Shihira, Y.; Sato, T.; Umemomto, H.; Tsunashima, S. *J. Chem. Soc., Faraday Trans.* **1993**, *89*, 995.
(32) Takayanagi, T.; Kurosaki, Y.; Sato, K.; Misawa, K.; Kobayashi, Y.; Tsunashima, S. *J. Phys. Chem. A* **1999**, *103*, 250.
(33) Takayanagi, T.; Kurosaki, Y.; Misawa, K.; Sugiura, M.; Kobayashi, Y.; Sato, K.; Tsunashima, S. *J. Phys. Chem. A* **1998**, *102*, 6251.
(34) Kobayashi, H.; Takayanagi, T.; Yokoyama, K.; Sato, T.; Tsunashima, S. *J. Chem. Soc., Faraday Trans.* **1995**, *91*, 3771.
(35) Kurosaki, Y.; Takayanagi, T.; Sato, K.; Tsunashima, S. *J. Phys. Chem. A* **1998**, *102*, 254.
(36) Takayanagi, T.; Kurosaki, Y.; Sato, K.; Tsunashima, S. *J. Phys. Chem. A* **1998**, *102*, 10391.
(37) Pederson, L. A.; Schatz, G. C.; Ho, T.-S.; Hollebeek, T.; Rabitz, H.; Harding, L. B.; Lendvay, G. *J. Chem. Phys.* **1999**, *110*, 9091.

(38) Sugawara, K.; Ishikawa, Y.; Sato, S. *Bull. Chem. Soc. Jpn.* **1980**, *53*, 1344.
(39) Sugawara, K.; Ishikawa, Y.; Sato, S. *Bull. Chem. Soc. Jpn.* **1980**, *53*, 3159.
(40) Butler, J. E.; Fleming, J. W.; Goss, L. P.; Lin, M. C. *Chem. Phys.* **1981**, *56*, 355.
(41) Berman, M. R.; Fleming, J. W.; Harvey, A. B.; Lin, M. C. *Chem. Phys.* **1982**, *73*, 27.
(42) Gosavi, R. K.; Safarik, I.; Strausz, O. P. *Can. J. Chem.* **1985**, *63*, 1689.
(43) Kajimoto, O.; Fueno, T. *Chem. Phys. Lett.* **1979**, *64*, 445.
(44) Kajimoto, O.; Yamasaki, H.; Fueno, T. *Chem. Phys. Lett.* **1979**, *68*, 127.
(45) Honma, K. *J. Chem. Phys.* **1993**, *99*, 7677.
(46) Tsurumaki, H.; Fujimura, Y.; Kajimoto, O. *Chem. Phys. Lett.* **1999**, *301*, 145.
(47) Umemoto, H. Private communication.
(48) Isaacson, A. D.; Truhlar, D. G.; Rai, S. N.; Stecker, R.; Hancock, G. C.; Garrett, B. C.; Redmon, M. J. *Comput. Phys. Commun.* **1987**, *47*, 21.
(49) Frisch, M. J.; Trucks, G. W.; Schlegel, H. B.; Gill, P. M. W.; Johnson, B. G.; Robb, M. A.; Cheeseman, J. R.; Keith, T.; Petersson, G. A.; Montgomery, J. A.; Raghavachari, K.; Al-Laham, M. A.; Zakrezewski, V. G.; Ortiz, J. V.; Foresman, J. B.; Cioslowski, J.; Stefanov, B. B.; Nanayakkara, A.; Challacombe, M. C.; Peng, Y.; Ayala, P. Y.; Chen, W.; Wong, M. W.; Andres, J. L.; Replogle, E. S.; Gomperts, R.; Martin, R. L.; Fox, D. J.; Binkley, J. S.; Defrees, D. J.; Baker, J.; Stewart, J. P.; Head-Gordon, M.; Gonzalez, C.; Pople, J. A. *Gaussian 94*; Gaussian, Inc.: Pittsburgh, PA, 1995.
(50) Dupuis, M.; Watts, J. D.; Villar, H. O.; Hurst, G. J. B. HONDO, Version 7; *Comput. Phys. Commun.* **1989**, *52*, 415.
(51) Herzberg, G. *Molecular Spectra and Molecular Structure II. Infrared and Raman Spectra of Polyatomic Molecules*; D. Van Nostrand Co.: New Jersey, 1945.
(52) Troe, J. *J. Chem. Phys.* **1977**, *66*, 4758.
(53) Johnston, H. S. *Gas-Phase Reaction Rate Theory*; The Ronald Press Co: New York, 1966.
(54) Schatz, G. C.; McCabe, P.; Connor, J. N. L. *Faraday Discuss.* **1998**, *110*, 139.
(55) Okabe, H. *Photochemistry of Small Molecules*; John Wiley & Sons: New York, 1978.
(56) Gemein, B.; Peyerimhoff, S. D. *J. Phys. Chem.* **1996**, *100*, 19257.
(57) Yamaguchi, Y.; Vacek, G.; Schaefer III, H. F. *Theor. Chim. Acta* **1993**, *86*, 97.